Anionic and cationic pollutants degradation via TiO$_2$ nanoleafed nanorods

Shervin Daneshvar e Asl [*], Sayed Khatiboleslam Sadrnezhaad

Advanced Bionanomaterials Laboratory, Department of Materials Science and Engineering, Sharif University of Technology, Azadi Avenue, PO Box 11155-9466, Tehran, Iran

A B S T R A C T

Hierarchical TiO$_2$ nanoleafed nanorod thin film was successfully synthesized on the fluorine doped tin oxide glass substrate. For this purpose, the nanorods were coated on the TiO$_2$ seeded substrate via the hydrothermal method. Then, nanoleafs were grown on the nanorods by aqueous chemistry. Field emission scanning electron microscopy, energy dispersive spectroscopy, and Raman spectroscopy were utilized for thin film characterization. The results clarified that anatase-phase nanoleafs were uniformly grown on the rutile-phase nanorods in the TiO$_2$ coating. The photocatalytic performance of the thin film was determined by photodegradation of anionic and cationic organic pollutants, and the photocatalytic decomposition mechanisms of the dyes were discussed. The improved photocatalytic activity of TiO$_2$ was ascribed to the photogenerated charges separation at the interface of rutile-nanorod/anatase-nanoleafs junctions and favorable light harvesting.

1. Introduction

Advanced oxidation processes (AOPs) have found great attention in the environmental remediation [1]. Among AOPs, heterogeneous photocatalysis is destructive technology resulting in the total degradation of most of the organic pollutants [2–8]. The solid semiconductor in powder or film form, oxygen as the electron scavenger and light as the energy source are involved in this process. As a result of light irradiation with an energy higher than that of semiconductor band-gap, the filled valence band electrons of semiconductor are excited to the unoccupied conduction band, and the positively charged holes remain in it. The electron-hole pairs would result in the incidence of the oxidation-reduction reactions on the photocatalyst surface [9–11].

The high oxidative potential of photogenerated holes on the TiO$_2$ surface caused it to be the most useable photocatalyst in the photooxidation of pollutant degradation [2,12]. Moreover, TiO$_2$ has some important superiorities including being environmentally friendly, photocorrosion resistance, thermal/chemical stability, availability and low cost [13–19].

Dyestuffs are a principal category of organic pollutants that lead to incrementing environmental danger. A significant percentage (about 15%) of the global production of dyes is lost within the dyeing process and is introduced to the textile effluents [20]. The release of dye included wastewaters in the ecosystem is the main source of perturbations in aquatic life, eutrophication, and non-aesthetic pollution [21].

So, the removal of dyes is an important challenge in the world. The photocatalytic degradation of dyes is an effective method for the purification of dye effluents [22–24].

In this work, a thin film of TiO$_2$ nanoleafed nanorods (NLNRs) on fluorine doped tin oxide glass (FTO) was synthesized, and the photocatalytic performance of this novel nanostructure for photodegradation of methyl orange and Rhodamine B was evaluated. Appropriate mechanisms were proposed for the photocatalytic degradation of the anionic and the cationic dyes used in this research.

2. Materials and method

2.1. Materials

Fluorine doped tin oxide glass was bought from Dyesol Company. Titanium tetrachloride, titanium butoxide, sodium chloride, 2-propanol, acetone, and hydrochloric acid were purchased from Merck. Boric acid, ammonium hexafluo-rotitanate, Rhodamine B, and methyl orange were bought from Sigma-Aldrich. The grade of water used in all stages was deionized water. All reagents were of analytical-grade and used as received, without further purification.

2.2. Synthesis

Hierarchical TiO2 nanoleafed nanorod thin film was synthesized on

---
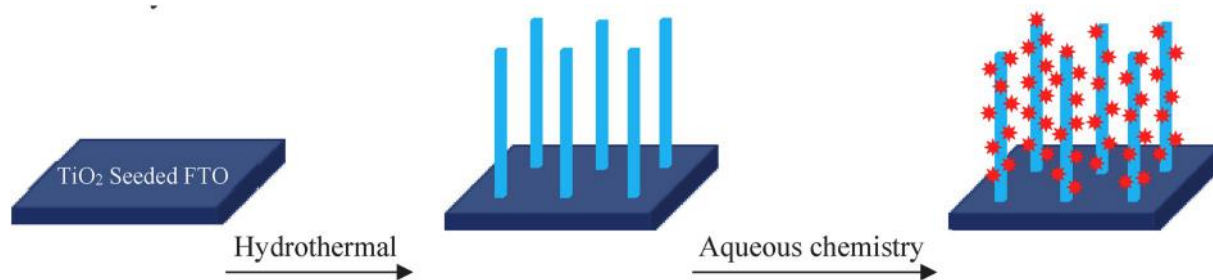
Scheme 1. Synthesis steps of hierarchical TiO₂ nanoleafed nanorod thin film.
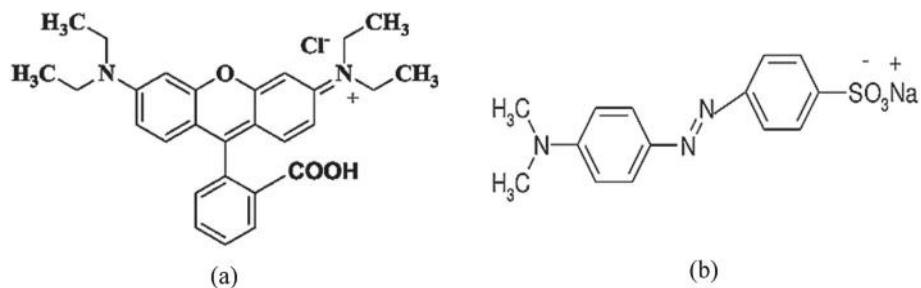

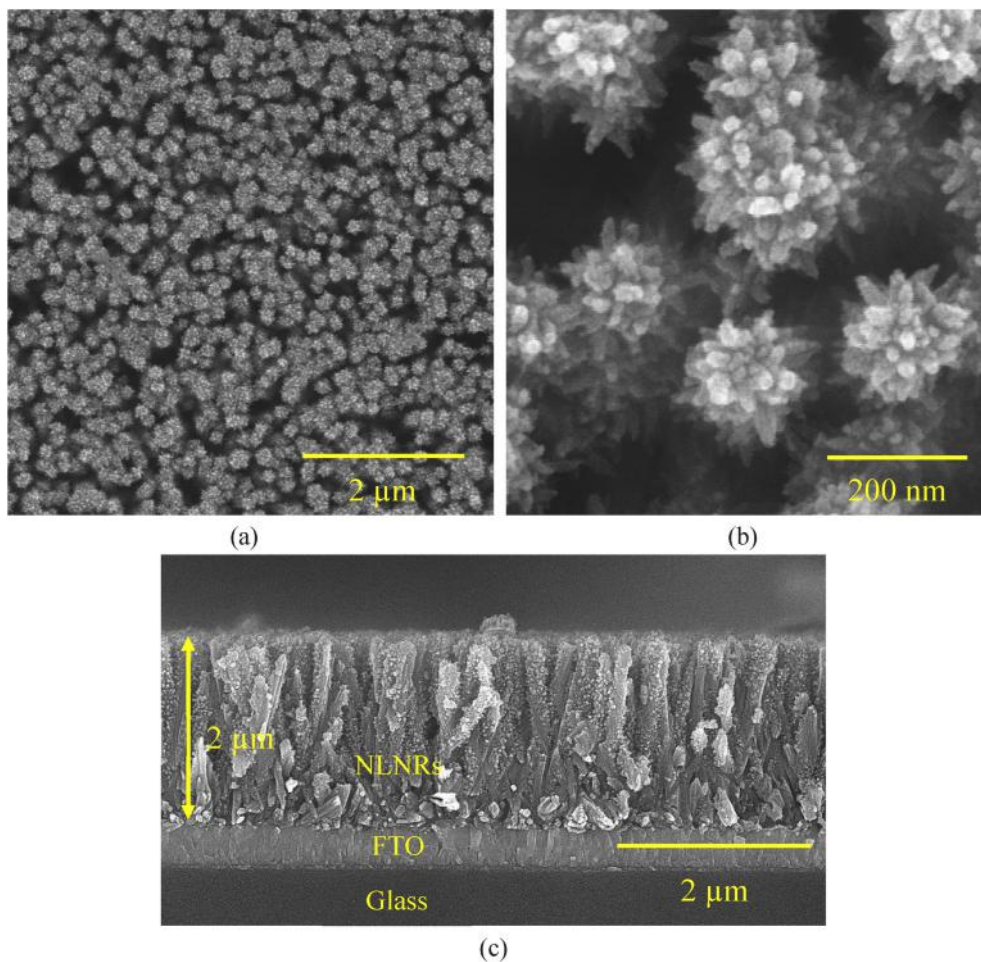**Fig. 1.** Molecular structures of (a) Rhodamine B and (b) methyl orange.

Fig. 2. FESEM images of (a) and (b) the thin film surface consisted of TiO₂ nanoleafed nanorods in two magnifications and (c) cross-sectional view of the thin film.
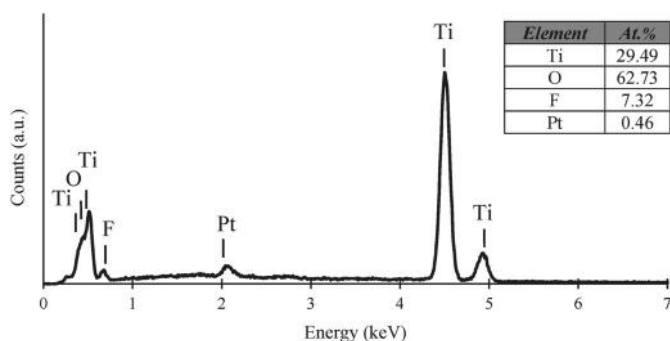
Fig. 3. Energy diffraction spectrum and elemental combination of TiO$_2$ nanoleafed nanorod thin film.

FTO according to our previous work [25], as shown in Scheme 1. At first, a TiO2 seed layer was coated on FTO by TiCl4 treatment. Then, rutile TiO2 nanorod arrays was synthesized via the hydrothermal method, and finally anatase TiO2 nanoleafs were grown by aqueous chemistry.

2.3. Photocatalytic performance test

The photocatalytic performance of TiO$_2$ nanoleafed nanorod thin film in the dye decomposition was determined via following method. The thin film (25 × 25 mm × mm in size) was put in 5 μM dye solution (Rhodamine B or methyl orange) in a water jacketed reactor under irradiation and dye concentration was measured at 15-min intervals up to 90 min. Prior to illumination to achieve the equilibrium absorption level, the reactor was left in darkness for 4 h. The dye solution was in contact with air during the test and agitated by a magnetic stirrer. The photocatalytic test was carried out three times, and the mean values were utilized for plotting the curves. Also, the thin film of TiO$_2$ nanorod arrays was used as the benchmark. Molecular structure of Rhodamine B and methyl orange are shown in Fig. 1.

Dye photodegradation curve via photocatalytic thin film can be fitted with pseudo-first-order kinetic according to Langmuir–Hinshelwood model [26]:

$$Ln\ (c_0/c) = kt \quad (1)$$

In Eq. (1), c_0 is the initial dye concentration at t = 0 (after absorption in darkness), c is its concentration after illumination for a duration of t > 0, and k is the reaction rate constant.

2.4. Instrumentations and characterizations

Field emission scanning electron microscope (FESEM; MIRA3TESCAN-XMU) was used for observation of TiO$_2$ thin film morphology. Besides, an energy dispersive spectroscope (EDS; JEOL JED-2300) installed to the FESEM was utilized to examination of the chemical stoichiometry of thin film. A Horiba Jobin Yvon modular Raman spectrometer equipped with a Stellar Pro Argon-ion laser operating at 514 nm with an incident power of 50 mW was applied to evaluating thin film crystalline phase. A Hitachi UH5300 double beam spectrophotometer was employed for monitoring the concentration changes of Rhodamine B and methyl orange solutions with the illumination time, by determining the absorbance at the wavelength of 554 nm and 464 nm, respectively. PLS-SXE300UV300 was used as the light source in photocatalytic experiments.

3. Results and discussion

FESEM images of TiO$_2$ nanoleafed nanorod thin film are shown in Fig. 2. The image of the thin film surface indicates that the coating has covered the entire surface of the FTO substrate monotonously and it is
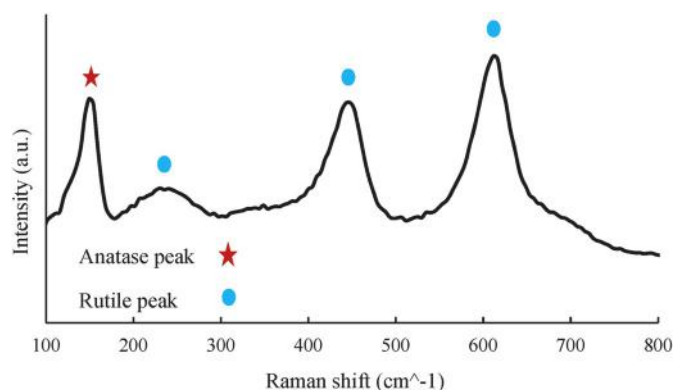

Fig. 4. Raman spectrum of TiO$_2$ nanoleafed nanorod thin film.

crack-free. As it is obvious, nanoleafs have grown uniformly on the surface of nanorods. The cross-sectional view presents that the coating has a thickness of about 2 μm. This nanostructure, due to the large specific surface area, possesses improved capability of light harvesting and the generation of charge carriers, which is an important advantage in promoting photocatalytic activity [27].

Energy diffraction spectrum and elemental composition of TiO$_2$ nanoleafed nanorod thin film are demonstrated in Fig. 3. The atomic ratio of Ti to O in the coating is approximately one-half. Oxygen adsorption on the thin film surface probably results in observation of excess oxygen in the thin film. Fluorine doping in the structure by replacement with O^{2-} ions during the step of nanoleafs growth, is feasible reason for the presence of this element in the spectrum. Titanium precursor, i.e., ammonium hexafluo-rotitanate, is responsible for providing fluorine. The platinum element has covered the thin film during the sample preparation for FESEM imaging.

Raman spectrum of TiO$_2$ nanoleafed nanorod thin film is illustrated in Fig. 4. As it is obvious, four peaks in 161 cm^{-1}, 245 cm^{-1}, 442 cm^{-1}, and 609 cm^{-1} appear in the spectrum which the first one is anatase characteristic peak and three other are rutile characteristic peaks. In fact, according to our previous work [8], the thin film is a biphasic hierarchical nanostructure, and anatase-phase nanoleafs are grown on the rutile-phase nanorods.

Photodegradation curves of Rhodamine B and methyl orange in the absence and presence of TiO$_2$ thin films and fitting results assuming a pseudo-first order reaction are indicated in Fig. 5. In the absence of TiO$_2$, 8% of Rhodamine B and 6% of methyl orange are decomposed after 90 min. As it is clear, synthesized TiO$_2$ thin films have better performance in decomposition of cationic dye than anionic one. On the other hand, TiO$_2$ nanoleafed nanorods display enhanced photocatalytic activity compared with TiO$_2$ nanorods.

Under light irradiation, the degradation of dye in aqueous solution occurs in two pathways in the presence of TiO$_2$ photocatalyst:

(a) Photocatalytic pathway: Titania absorbs photons with higher energy than that of its band-gap, and electron-hole pairs are generated by electrons exciting from TiO$_2$ valence band to its conduction band. Some of e$^-$/h$^+$ pairs undergo recombination while others migrate to the surface of the TiO$_2$ to lead to photocatalytic reactions. The produced holes may be trapped by the hydroxyl groups adsorbed on TiO$_2$ surface and result in the hydroxyl radicals formation. Electrons can also be trapped by oxygen and lead to the production of superoxide radicals. The holes, along with hydroxyl and superoxide radicals, oxidize dye in aqueous solution to carbon dioxide, water, and some simple mineral acids. These events are summarized in the reaction (1) to (4):
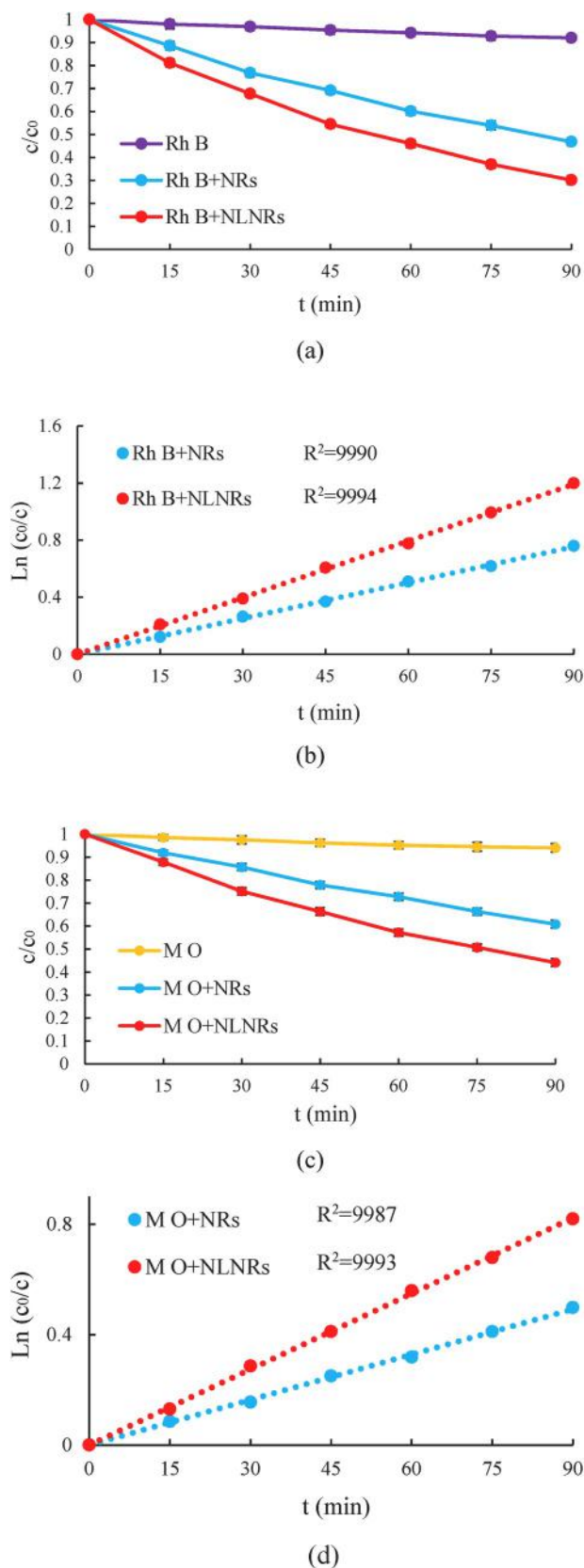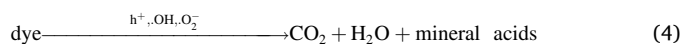
$$TiO_2 + h\upsilon \rightarrow TiO_2(e^- + h^+) \quad (1)$$

$$h^+ + OH^- \rightarrow .OH \quad (2)$$

(a)

(b)

(c)

(d)
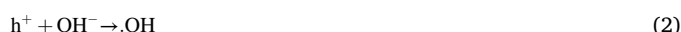
Fig. 5. Photodegradation curves of (a) Rhodamine B and (c) methyl orange by TiO$_2$ thin films. (b) and (d) fitting results assuming a pseudo-first order reaction for (a) and (c), respectively. (For interpretation of the references to colour in this figure legend, the reader is referred to the Web version of this article.)
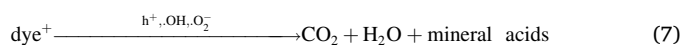
Table 1

The rate constants of the photodegradation reactions of Rhodamine B and methyl orange by TiO$_2$ thin films (k, min^{-1}).
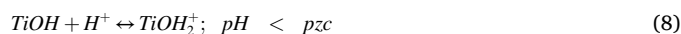
TiO$_2$ thin films	Nanoleafed nanorods	Nanorods
Rhodamine B	1.31×10^{-2}	0.83×10^{-2}
Methyl orange	0.92×10^{-2}	0.54×10^{-2}

$$e^- + O_2 \rightarrow .O_2^- \tag{3}$$

$$dye \xrightarrow{\quad h^+,.OH,.O_2^- \quad} CO_2 + H_2O + mineral\ acids \tag{4}$$

(b) Photosensitization: The absorbed dye on the surface of the titania is excited by light, and inject electron to TiO$_2$ conduction band. As a result, the cationic dye radical forms. Electrons injected to the TiO$_2$ conduction band produce superoxide radicals according to reaction (3). Then, dye is broken down into final products. This process is mainly a surface reaction and occurs on the surface of titania [28]. These events are summarized in the reaction (5) to (7):

$$dye + h\upsilon \rightarrow dye^* \tag{5}$$

$$dye^* + TiO_2 \rightarrow dye^+ + TiO_2(e^-) \tag{6}$$

$$dye^+ \xrightarrow{\quad h^+,.OH,.O_2^- \quad} CO_2 + H_2O + mineral\ acids \tag{7}$$

The point of zero charge (PZC) of the synthesized nanostructures is 5.9. Therefore, the surface charge of the coating in the aqueous solution of dyes is as follows:

$$TiOH + H^+ \leftrightarrow TiOH_2^+; \quad pH \quad < \quad pzc \tag{8}$$

$$TiOH + OH^- \leftrightarrow TiO^- + H_2O; \quad pH \quad > \quad pzc \tag{9}$$

According to reaction (9), the synthesized thin films has the negative surface charge at the neutral acidity of photocatalytic tests (pH~7). Thus, given that methyl orange has an anionic configuration, it adsorbs to a little extent on the surface of titania, and pathway (a) is merely effective degradation route. Accordingly, synthesized thin films represent better performance in decomposition of cationic dye than anionic one.

There are three reasons for photocatalytic activity improvement in TiO$_2$ nanoleafed nanorods in comparison with TiO$_2$ nanorod thin film: (1) Biphasic structure of the former one causes in electron transfer from rutile to anatase [29], and as a result, charge separation enhancement, (2) nanoleafed nanorods have a higher light harvesting ability due to larger surface area [8], and (3) tendency between oxygen and surface of anatase is higher than that of rutile, and therefore, anatase is more effective in oxygen reduction via the photogenerated electrons [30].

The rate constants of the photodegradation reactions of Rhodamine B and methyl orange by TiO$_2$ thin films under light irradiation are summarized in Table 1.

4. Conclusion

Hierarchical rutile/anatase TiO$_2$ nanorod/nanoleafs thin film was successfully synthesized. Photocatalytic performance of this novel nanostructure in photodegradation of cationic and anionic dyes was measured and discussed. The enhanced photocatalytic activity of TiO$_2$ was ascribed to great specific surface area, favorable light harvesting, and the photogenerated charges separation at the interface of rutile-nanorod/anatase-nanoleafs junctions. Because of the thin film had the negative surface charge at the neutral acidity of tests, it shown better photocatalytic performance in case of cationic dye photodegradation.

Declaration of competing interest

The authors declare that they have no known competing financial

interests or personal relationships that could have appeared to influence the work reported in this paper.

Acknowledgments

This work was supported by the Iran National Science Foundation, Iran's National Elites Foundation, and Iran Nanotechnology Initiative Council.

Appendix A. Supplementary data

Supplementary data to this article can be found online at https://doi.org/10.1016/j.solidstatesciences.2020.106263.

References

[1] S. Parsons (Ed.), Advanced Oxidation Processes for Water and Wastewater Treatment, IWA publishing, 2004.

[2] M.A. Fox, M.T. Dulay, Heterogeneous photocatalysis, Chem. Rev. 93 (1993) 341–357.

[3] A. Fujishima, X. Zhang, D.A. Tryk, Heterogeneous photocatalysis: from water photolysis to applications in environmental cleanup, Int. J. Hydrogen Energy 32 (2007) 2664–2672.

[4] A.O. Ibhadon, P. Fitzpatrick, Heterogeneous photocatalysis: recent advances and applications, Catalysts 3 (2013) 189–218.

[5] J.A. Byrne, P.S.M. Dunlop, J.W.J. Hamilton, P. Fernández-Ibáñez, I. Polo-López, P. K. Sharma, A.S.M. Vennard, A Review of heterogeneous photocatalysis for water and surface disinfection, Molecules 20 (2015) 5574–5615.

[6] S.N. Ahmed, W. Haider, Heterogeneous photocatalysis and its potential applications in water and wastewater treatment: a review, Nanotechnology 29 (2018) 342001–342030.

[7] U.I. Gaya, A.H. Abdullah, Heterogeneous photocatalytic degradation of organic contaminants over titanium dioxide: a review of fundamentals, progress and problems, J. Photochem. Photobiol. C Photochem. Rev. 9 (2008) 1–12.

[8] S. Daneshvar e Asl, S.K. Sadrnezhaad, Photocatalytic activity of rutile/anatase TiO_2 nanorod/nanobranch thin film loaded with Au@Ag@Au core double shell nanoparticles, J. Photochem. Photobiol. Chem. 380 (2019) 111843–118851.

[9] B. Ohtani, Preparing articles on photocatalysis— beyond the illusions, misconceptions, and speculation, Chem. Lett. 37 (2008) 217–229.

[10] R. Fagan, D.E. McCormack, D.D. Dionysiou, S.C. Pillai, A review of solar and visible light active TiO_2 photocatalysis for treating bacteria, cyanotoxins and contaminants of emerging concern, Mater. Sci. Semicond. Process. 42 (2016) 2–14.

[11] R. Leary, A. Westwood, Carbonaceous nanomaterials for the enhancement of TiO_2 photocatalysis, Carbon N. Y. 49 (2011) 741–772.

[12] M.R. Hoffmann, S.T. Martin, W. Choi, D.W. Bahnemannt, Environmental applications of semiconductor photocatalysis, Chem. Rev. 95 (1995) 69–96.

[13] D. Shi, Z. Guo, N. Bedford, Nanotitanium oxide as a photocatalytic material and its application. Nanomater. Devices, first ed., Elsevier, United States, 2015, pp. 161–174.

[14] C. Su, C.-M. Tseng, L.-F. Chen, B.-H. You, B.-C. Hsu, S.-S. Chen, Sol–hydrothermal preparation and photocatalysis of titanium dioxide, Thin Solid Films 498 (2006) 259–265.

[15] Y. Wang, Y. Huang, W. Ho, L. Zhang, Z. Zou, S. Lee, Biomolecule-controlled hydrothermal synthesis of C–N–S-tridoped TiO_2 nanocrystalline photocatalysts for NO removal under simulated solar light irradiation, J. Hazard Mater. 169 (2009) 77–87.

[16] M. Pelaez, P. Falaras, V. Likodimos, A.G. Kontos, A.A. de la Cruz, K. O'Shea, D. D. Dionysiou, Synthesis, structural characterization and evaluation of sol–gel-based NF-TiO_2 films with visible light-photoactivation for the removal of microcystin-LR, Appl. Catal. B Environ. Environ. 99 (2010) 378–387.

[17] P. Swarnakar, S.R. Kanel, D. Nepal, Y. Jiang, H. Jia, L. Kerr, M.N. Goltz, J. Levy, J. Rakovan, Silver deposited titanium dioxide thin film for photocatalysis of organic compounds using natural light, Sol. Energy 88 (2013) 242–249.

[18] J.M. Poyatos, M.M. Muñio, M.C. Almecija, J.C. Torres, E. Hontoria, F. Osorio, Advanced oxidation processes for wastewater treatment: state of the art, Water Air Soil Pollut. 205 (2010) 187–204.

[19] C. Comninellis, A. Kapalka, S. Malato, S.A. Parsons, I. Poulios, D. Mantzavinos, Advanced oxidation processes for water treatment: advances and trends for R&D, J. Chem. Technol. Biotechnol. 83 (2008) 769–776.

[20] H. Zollinger, Color Chemistry: Syntheses, Properties, and Applications of Organic Dyes and Pigments, John Wiley & Sons, 2003.

[21] A. Houas, H. Lachheb, M. Ksibi, E. Elaloui, C. Guillard, J. Herrmann, Photocatalytic degradation pathway of methylene blue in water, Appl. Catal. B Environ. 31 (2001) 145–157.

[22] M.A. Rauf, S.S. Ashraf, Fundamental principles and application of heterogeneous photocatalytic degradation of dyes in solution, Chem. Eng. J. 151 (2009) 10–18.

[23] R. Molinari, F. Pirillo, M. Falco, V. Loddo, L. Palmisano, Photocatalytic degradation of dyes by using a membrane reactor, Chem. Eng. Process 43 (2004) 1103–1114.

[24] R.J. Tayade, P.K. Surolia, R.G. Kulkarni, R V Jasra, Photocatalytic degradation of dyes and organic contaminants in water using nanocrystalline anatase and rutile TiO_2, Sci. Technol. Adv. Mater. 8 (2007) 455–462.

[25] S. Daneshvar e Asl, A. Eslami Saed, S.K. Sadrnezhaad, Hierarchical rutile/anatase TiO_2 nanorod/nanoflower thin film: synthesis and characterizations, Mater. Sci. Semicond. Process. 93 (2019) 252–259.

[26] J.M. Wu, T.W. Zhang, Photodegradation of Rhodamine B in water assisted by titania films prepared through a novel procedure, J. Photochem. Photobiol. Chem. 162 (2004) 171–177.

[27] J. Wang, T. Zhang, D. Wang, R. Pan, Q. Wang, H. Xia, Improved morphology and photovoltaic performance in TiO_2 nanorod arrays based dye sensitized solar cells by using a seed layer, J. Alloys Compd. 551 (2013) 82–87.

[28] Y. Ma, J.-N. Yao, Photodegradation of Rhodamine B catalyzed by TiO_2 thin films, J. Photochem. Photobiol. Chem. 116 (1998) 167–170.

[29] D.O. Scanlon, C.W. Dunnill, J. Buckeridge, S.A. Shevlin, A.J. Logsdail, S. M. Woodley, C.R.A. Catlow, M.J. Powell, R.G. Palgrave, I.P. Parkin, G.W. Watson, T.W. Keal, P. Sherwood, A. Walsh, A.A. Sokol, Band alignment of rutile and anatase TiO_2, Nat. Mater. 12 (2013) 798–801.

[30] D. Tsukamoto, Y. Shiraishi, Y. Sugano, S. Ichikawa, S. Tanaka, T. Hirai, Gold nanoparticles located at the interface of anatase/rutile TiO_2 particles as active plasmonic photocatalysts for aerobic oxidation, J. Am. Chem. Soc. 134 (2012) 6309–6315.